WARSAW UNIVERSITY OF TECHNOLOGY Index 351733
FACULTY OF CIVIL ENGINEERING
COMMITTEE FOR CIVIL AND WATER ENGINEERING
POLISH ACADEMY OF SCIENCES ISSN 1230-2945
DOI: 10.24425/ace.2026.158630
ARCHIVES OF CIVIL ENGINEERING
Vol. LXXII ISSUE 2 2026
pp. 607 –621
© 2026. Tadeusz Zwoliński.
This is an open-access article distributed under the terms of the Creative Commons Attribution-NonCommercial-NoDerivatives License (CC BY-NC-ND 4.0, https://creativecommons.org/licenses/by-nc-nd/4.0/), which permits use, distribution, and reproduction in any medium, provided that the Article is properly cited, the use is non-commercial, and no modifications or adaptations are made.

**Research paper**

# Experimental studies on an extended end plate joint with prestressed bolts

**Tadeusz Zwoliński**[1]

**Abstract:** This paper presents the results of an experimental study of an extended end plate moment connection with prestressed bolts. Increments in bolt forces under loading were measured, as two solutions to eliminate those were compared. The first one consists of using a thick extended end plate to reduce prying action, the second one introduces a spacer plate to eliminate prying completely. Limiting increments in bolt forces is essential in the design of joints working under cyclic load, which can be prone to fatigue failure. Loss of preload was measured. Four types of connection setups were studied, two of which included a spacer plate installed between the extended end plate and a column flange. M16 grades 8.8 and 10.9 were used. The beam element was made of IPE 400 section, and the column element was made of HEB 220 section – both of S355-J2 grade steel. The possibility of using bolts not dedicated to prestress was explored. Finite Element Analysis using ANSYS Workbench software was performed. Results were summarised and discussed.

**Keywords:** bolt, prestress, FEM, ANSYS Workbench, spacer plate, prying

[1]MSc., Eng., Warsaw University of Technology, Faculty of Civil Engineering, Al. Armii Ludowej 16, 00-637 Warsaw, Poland, e-mail: tadeusz.zwolinski@pw.edu.pl, ORCID: 0000-0002-9973-0147

# 1. Introduction

Bolted joints are commonly used in steel structures, as they offer quick and easy assembly. Adding prestress to the bolts reduces the amplitude of forces in them, improving fatigue performance which often proved safety-critical. Moreover, the stiffness of the joint is thus improved. However, the design of such joints can be very laborious, especially when complex geometries and many bolts are involved, as shown in [1]. Accurate assessment of bolt forces, especially with prying accounted for, is critical for safe design and poses a significant challenge, as was shown in [2].

The first solution to address this issue is to increase the plate thickness, to reduce prying, as for thick plates, the through-thickness effects play a major role, not bending. Several recommendations can be found in literature and papers, for the minimal thickness of a plate, that reduces prying action, and can be used in prestressed connections:

Minimal thickness can be derived from the formulas in Table 6.2 of the Eurocode [3], as is also recommended in [4]:

$$t_{\min} \geq 2\sqrt{\frac{mF_{t.Rd}}{l_{\text{eff}} f_{y.p}}} \tag{1.1}$$

where: $m$ – bolt axis distance from the edge of the weld, $F_{t.Rd}$ – bolt design tensile strength, $l_{\text{eff}}$ – effective length of the plate, $f_{y.p}$ – yield strength of the plate.

In [5]:

$$t_{\min} \geq d\sqrt[3]{\frac{R_m}{1000}} \tag{1.2}$$

where: $d$ – bolt diameter, $R_m$ $[MPa]$ – bolt ultimate tensile strength.

In [6], for joints under dynamic loads, it is recommended to use:

$$t_{\min} \geq 1.25d\sqrt[3]{\frac{R_m}{1000}} \tag{1.3}$$

The above conditions provide different recommended thicknesses for the same joint, which can be quite confusing. The extended endplate used in this study is much thicker than required by the formulas Eq. (1.1), (1.2), and (1.3). The thickness of the extended end plate $t_p = 25$ mm, as well as column flange thickness $t_{f.c} = 16$ mm generally satisfies the above conditions. The only exception is $t_{f.c} < 1.25d\sqrt[3]{\frac{R_m}{1000}}$. The thickness of the column flange is relatively lesser than that, of an end plate, however, it has more support edges, and therefore its stiffness is similar to that, of an endplate. Therefore, it can be stated, that the joint should experience little to no prying.

The second solution is to install a spacer plate between the end plate and column flange, to eliminate prying completely, as the free ends of the plates could not touch at all (Fig. 7).

Next, the basic concepts of a prestressed bolted connection are discussed using the example of a T-stub. In Fig. 1, two types of behaviour can be seen, one joint with a thick plate, and the second with a thin one.

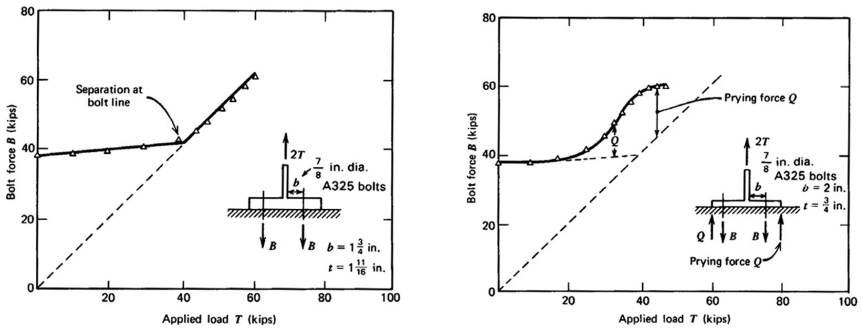


(a) (b)

Fig. 1. External load vs bolt force relation: (a) thick plate, (b) thin plate [7]

The point at which the bolt force starts to increase rapidly is called the point of separation, that is when the plates come apart, and compression between them comes to zero (Fig. 1a). Once this happens, the joint no longer satisfies the design condition for serviceability limit state. As can be seen in Fig. 1a, there is an increment in bolt force before this, mainly due to through thickness effects, and little from the prying force, as described by Eq. (1.5). This increase can be within 20% [8]. In [9], one can find values ranging from 5–10% for most typical cases. This is how the studied connections in cases A and B (without the spacer plate) are expected to behave. Joints in cases C and D are also expected to behave this way, as no prying is involved. For a thin plate though (Fig. 1b), the force increase before the point of separation is more profound. This is mainly due to prying, and little due to through thickness effects. The theoretical point of separation for types A and C examined in this study is when $N_{0.1}$ = 153 kN and $N_{0.1}$ = 192 kN for types B and D (bolt row 1). Derivation of these values is explained in Section 5. After this point, the joint behaves as if it was not prestressed. Before that point, the increment in bolt force $\Delta F_i$ depends on the stiffness ratio of the components in the joint, and can be described below.

For types C and D:

$$\Delta F_i = F_i \frac{k_1}{k_1 + k_{sp}} \tag{1.4}$$

where: $\frac{1}{k_1} = \frac{1}{k_{\text{bolt}}} + \frac{1}{k_{f.c}} + \frac{1}{k_{e.p}}$

For types A and B:

$$\Delta F_i = F_i \frac{k_{\text{bolt}}}{k_{\text{bolt}} + k_{\text{plate}}} + Q_i \tag{1.5}$$

where: $Q_i$ – prying force. Many attempts to estimate the value of prying force have been made.

Some examples are cited below:

$$Q_i = \left( \frac{3m}{8n} - \frac{t^3}{328} \right) F_i \quad \text{(SI Units)} \tag{1.6}$$

as suggested by Douty and McGuire, described in [7], where $m$ – distance of the bolt axis from the load axis, $t$ – plate thickness, $n$ – distance of the bolt axis to the axis of the prying force.

$$Q_i = F_i \left( \frac{100bd^2 - 18wt^2}{70ad^2 + 21wt^2} \right) \tag{1.7}$$

from analytical and experimental study at the University of Illinois in [10] where $b$ – distance of the bolt axis from the load axis, $d$ – bolt diameter, $w$ – effective width of the plate, $t$ – plate thickness, $a$ – distance of the bolt axis to the axis of the prying force. One more proposal is:

$$Q_i = \frac{b}{2n} \left( F_i - \frac{p_0 w t^4}{27nb^2} \right) \tag{1.8}$$

from [11], where $b$ – distance of the bolt axis to the most heavily loaded section in bending, $w$ – effective width of the plate, $t$ – plate thickness, $n$ – distance of the bolt axis to the axis of the prying force, $p_0$ – minimum proof stress of the bolt.

Other symbols used in Eq. (1.4) and Eq. (1.5) are described below: $k_{\text{bolt}} = \dfrac{EA_{\text{bolt}}}{l_s}$ – bolt axial stiffness, where $E$ – Young modulus, $A_{\text{bolt}}$ – bolt cross-section area $l_s$ – bolt effective length, $k_{sp}$ – spacer plate axial stiffness, $k_{f.c}$ – column flange stiffness in bending, $k_{e.p}$ – end plate stiffness in bending, $k_{\text{plate}}$ – plate stiffness under compression, according to [12], $F_i$ – external force acting on a bolt, $\Delta F_i$ – increment in bolt force, added to the initial prestress load.

# 2. Materials and methods

## 2.1. Specimens

All steel elements apart from the bolts were made from typical S355J2-grade steel [13]. The beam element was made with an IPE 400 section and the column element was made with a HEB 220 section. Ribs and end plates were welded with fillet welds, and their thickness was such, that the strength of the weld was equal to or greater than that of the joined elements. It should be acknowledged that normally this joint would require M24 grade 8.8 or 10.9 bolts to provide adequate strength and be applied in a real structure. Therefore, the beam, column, end plate and ribs were overdesigned in comparison to the bolts. This was done to ensure that these elements work within the elastic range, and therefore strained bolts can be replaced with new ones after testing. Otherwise, such a joint could only be tested once, with one set of bolts.

## 2.2. Bolts

In all tests, M16 bolts were used. Two types of bolts were used (Fig. 2) – regular, fully threaded 8.8-grade bolts [14], [15], and partially threaded bolts for prestress of 10.9-grade [16]. Bolt characteristics are presented in Table 1. where: $l$ – shank length, $k$ – head height, $m$ – nut height, $d$ – diameter, $s$ – nut width, $h$ – washer height, $d_2$ – washer width, $b$ – length of the threaded part, $A_s$ – effective area of the threaded part, $f_{yb}$ – bolt yield strength, $f_{ub}$ – bolt ultimate strength.

Table 1. Properties of the bolts

| | $l$ [mm] | $k$ [mm] | $m$ [mm] | $d$ [mm] | $s$ [mm] | $h$ [mm] | $d_2$ [mm] | $b$ [mm] | $A_s$ [mm$^2$] | $A$ [mm$^2$] | $f_{yb}$ [MPa] | $f_{ub}$ [MPa] |
|---|---|---|---|---|---|---|---|---|---|---|---|---|
| **8.8** | 100 | 10 | 14.8 | 16 | 24 | 3 | 30 | — | 157 | -- | 640 | 800 |
| **10.9** | 100 | 10 | 13 | 16 | 27 | 4 | 30 | 38 | 157 | 201 | 900 | 1000 |

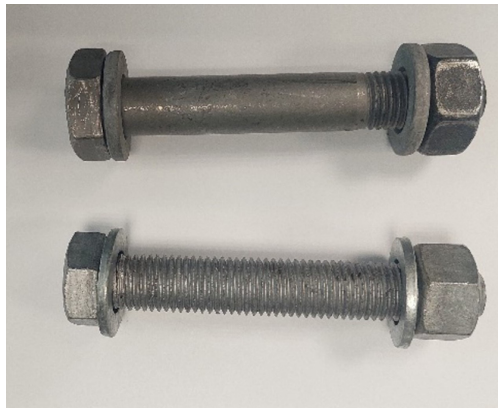

Fig. 2. 10.9 with partial thread and 8.8 fully threaded bolts

## 2.3. Torque wrench

A calibrated torque wrench was used to prestress the bolts (Fig. 3). It could generate up to 210 Nm torque. Alongside, an angle meter was used, to control the rotation of the nut.


Fig. 3. Torque wrench with an angle meter

## 2.4. Force sensor

To monitor bolt forces, 2 strain-gage-based sensors (Fig. 4) were used [17]. The measuring range was up to 200 kN with 1% accuracy. A big advantage of these sensors was the ability to constantly monitor bolt force, which allowed accurate prestress. Also, they could be reused for every test. Sensor basic dimensions are: outer diameter: 48 mm, inner diameter: 16 mm, thickness: 10 mm.

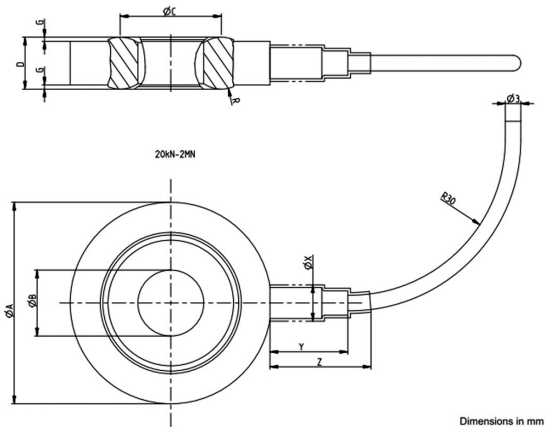


Fig. 4. Force sensor [17]

## 2.5. Hydraulic press

The tests were conducted in a hydraulic press (Fig. 5), that works axially and can generate up to 1000 kN of force. During the testing, displacement is controlled, with a rate of 0.05 mm/sec. The maximum displacement of a cylinder is 400 mm. Length adapters are used to adjust for the length of the test specimen.

Fig. 5. Hydraulic press

## 2.6. Test specimen

The test specimen consisted of 8 bolts that carried the load (Fig. 6). The two bottom bolts were located in the compression zone, and were not subjected to a lot of tension, therefore were not subject of interest. At the top, 6 bolts carried tensile load from the bending moment. The thickness of the extended end plate is $t_p = 25$ mm, and for column flange thickness $t_{f.c} = 16$ mm. As for the spacer plate – it had a thickness $t_{sp} = 10$ mm, and had an exact geometry of a IPE 400 beam, as can be seen in Fig. 7b). The test setup can be seen in Fig. 8.

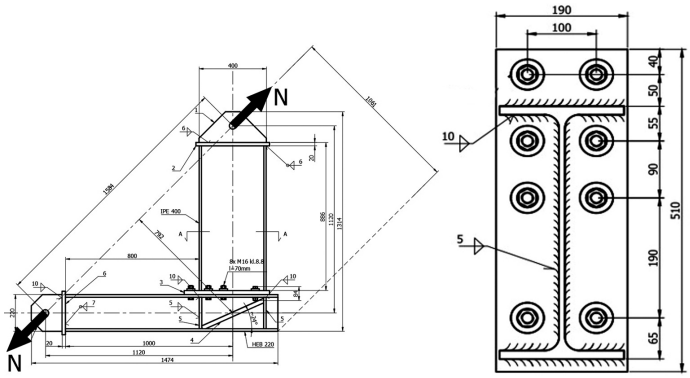


Fig. 6. Specimen dimensions and extended end plate joint detail

Fig. 7. (a) Joint with a spacer plate installed, (b) spacer plate

Fig. 8. Specimen after installation in the hydraulic press with force sensors installed

# 3. Testing procedure

## 3.1. Introduction

Four types of joint were tested:

– **Type A**: with 8.8 grade bolts without a spacer plate,
– **Type B**: with 10.9 grade bolts without a spacer plate,
– **Type C**: with 8.8 grade bolts with a spacer plate,
– **Type D**: with 10.9 grade bolts with a spacer plate.

It was decided to overload the joint with an external force $N = 1.55N_{0.1}$, that is for types A and C $N = 1.55N_{0.1} = 237$ kN and for types B and D $N = 1.55N_0 = 300$ kN, but not to exceed the bolt tensile capacity, as it could damage the sensors. $N_{0.1}$ is the value of external load (see Fig. 6) that generates bolt force equal to that of prestress (for row 1). This is described in detail in Section 5.

## 3.2. Prestressing of the bolts

Prestressing was performed with a torque wrench (Section 2.3), and the bolt threads were treated with a MoS2 molybdenum grease. The desired prestress loads were: $F_0 = F_{p.C} = 88$ kN for types A and C and $F_0 = F_{p.C} = 110$ kN for type B and D. All the bolts were initially prestressed with a torque, as in [8]:

$$M = 0.75 \cdot 0.13 d F_{p.C}$$

For Types A and C this is:

$$M = 0.75 \cdot 0.13 \cdot 16 \text{ mm} \cdot 88000 \text{ N} = 137 \text{ N} \cdot \text{m}$$

For Types B and D this is:

$$M = 0.75 \cdot 0.13 \cdot 16 \text{ mm} \cdot 110000 \text{ N} = 172 \text{ N} \cdot \text{m}$$

The second phase consisted of nut rotation with a predetermined angle. Recommended values of rotation angles can be found in [11], [8]. However, these recommendations can be considered as approximations, as the same angle is used for a variety of bolt types. Therefore, an accurate value of the angle of rotation was established experimentally, with the help of a force sensor (Section 2.4). The result was considered valid when the same force of prestress was achieved twice in a row for one bolt. Once the prestress procedure for one bolt was perfected, sensors were placed on different bolts, and the procedure was repeated. This allowed corrections to be made, to achieve equal prestress in all the bolts, even those that were not equipped with sensors in the final test. The final prestress load of the bolts was within 5% tolerance of the desired value. The experimentally determined angles of rotation were:

- Type A – $\alpha = 60°$,
- Type B – $\alpha = 45°$,
- Type C – $\alpha = 46°$,
- Type D – $\alpha = 46°$.

## 3.3. Bolt strength tests

To establish the loading range of the specimen the real tensile strength of the bolts was verified first. Three samples of 8.8-grade bolts were tested, with the nut placed with 2 threads sticking outside. Three samples of 10.9 grade bolt were tested, where the nut was placed with 2 threads sticking outside. Minimum capacity of an 8.8-grade M16 bolt is equal to 125.6 kN, and for an M16 10.9 grade that is 163 kN, according to [18], and all the samples proved to have required strength.

# 4. Finite Element Analysis

Finite Element Analysis was performed for all four types of studied joints – A, B, C and D. Multilinear material model was used for steel S355-J2 grade, described in [19] and shown in Table 2. For bolts of grades 8.8 and 10.9, a bilinear material model was chosen, with tangent modulus $E_t$ = 2000 MPa.

Table 2. Stress-strain parameters for S355-J2 steel

| | $E$ [GPa] | $f_y$ [MPa] | $f_u$ [MPa] | $\varepsilon_y$ [%] | $\varepsilon_{sh}$ [%] | $\varepsilon_u$ [%] | $E_{sh}$ [MPa] | $C_1$ |
|---|---|---|---|---|---|---|---|---|
| S355-J2 | 210 | 355 | 490 | 0.17 | 1.74 | 16.53 | 2283 | 0.38 |

ANSYS Workbench software was used for the calculations. Element type SOLID 186 with quadratic displacement behaviour was chosen. Discretization was adjusted, so that the key elements in bending (column flange and end plate) were composed of 5 elements in the direction perpendicular to the plate surface. Frictional connections were applied to all contacts, Frictional connections were applied on all contacts, with a friction coefficient equal to 0.15. For contacts, a stiffness update after each iteration was chosen, to improve contact behaviour. In the first step, preload was applied to the bolts with a *load-lock* function. After that, the external load was applied using *remote displacement,* acting in points where the hydraulic press was fixed to the specimen. The only rotation allowed was that about the $z$-axis (Fig. 9). Symmetry plane was applied through the middle of the column web. Compression between plates in contact can be seen in Fig. 10.

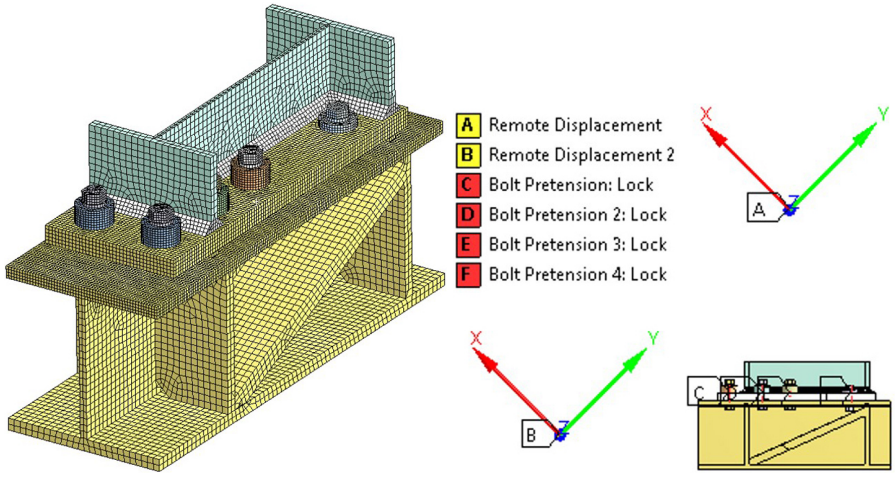


Fig. 9. (a) 3D model discretization, (b) support and load conditions

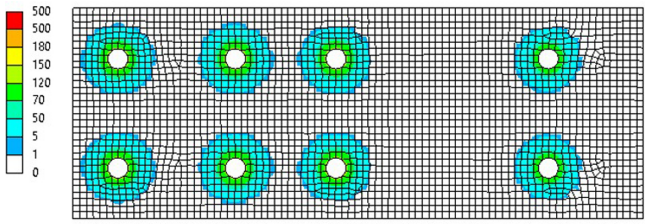


(a)

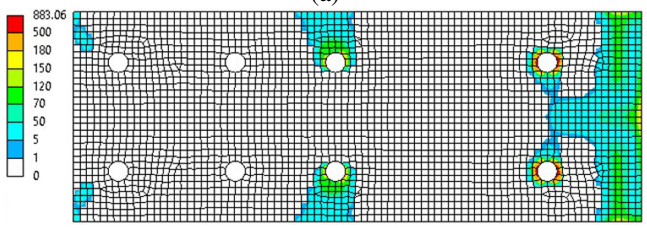


(b)

Fig. 10. Areas of compression between column flange and end plate for type D: (a) after prestressing, (b) at $N = 300$ kN

# 5. Test results

For comparative purposes, theoretical point of separation is calculated for the presented cases. It is a point when the external load $N$, generated by the hydraulic press creates axial tension in the bolt that is equal to the bolt prestress, as described in Eq. (5.1). This external load generates bending, tension and shear in the joint, and the loading scheme can be seen in Fig. 6. $N_{0.1}$ and $N_{0.2}$ are values of the external load that generate a tensile force in the bolts (row 1 and row 2 respectively), that is equal to the prestress load, so $F = F_0$:

$$F_F + F_M = F \tag{5.1}$$

where: $F_F$ – bolt force generated by external axial force $\dfrac{N}{\sqrt{2}}$ acting parallel to the beam axis.

For bolt row 1:

$$F_{F1} = \frac{(0.5 t_{f.b} b_{f.b})}{2A_b} \cdot \frac{N}{\sqrt{2}}$$

For bolt row 2:

$$F_{F2} = \frac{(0.5 t_{f.b} b_{f.b}) + 0.295 h_w t_w}{2A_b} \cdot \frac{N}{\sqrt{2}}$$

$t_{f.b}$ – thickness of the beam flange,
$b_{f.b}$ – width of the beam flange,
$h_w$ – height of the beam web,
$t_w$ – thickness of the beam web,
$A_b$ – area of the beam cross section,
$F_M$ – bolt force generated by external bending moment $N \cdot e$.

For bolt row 1:

$$F_{M1} = \frac{Ne}{2\left(h_1 + \frac{h_2^2}{h_1} + \frac{h_3^2}{h_1}\right)}$$

For bolt row 2:

$$F_{M2} = F_{M1}\frac{h_2}{h_1}$$

$h_1, h_2, h_3$ – distance of each bolt row measured from the center of compression zone, assumed to be located at $0.1h_b$ from the bottom edge of the beam compression flange.

$h_b$ – height of the beam,

$e$ – lever arm (Fig. 6),

$F_0$ – bolt prestress load,

$F$ – bolt force.

The Eq. (5.1) for bolt row 1 becomes:

$$0.051N_{0.1} + 0.522N_{0.1} = F \tag{5.2}$$

therefore, when $F = F_0$ $N_{0.1} = 1.746F_0$

For bolt row 2:

$$0.09N_{0.2} + 0.402N_{0.2} = F \tag{5.3}$$

therefore, when $F = F_0$ $N_{0.2} = 2.03F_0$

The theoretical point of separation for types A and C examined in this study is when $N_{0.1} = 153$ kN and $N_{0.1} = 192$ kN for types B and D (bolt row 1). For bolt row 2 $N_{0.2} = 178$ kN for types A and C, and $N_{0.2} = 223$ kN for types B and D. Now, the real bolt forces from the experiment, as well as from FEM are compared against external load $N$ in Fig. 11 and Fig. 12. Eq. (5.2) and Eq. (5.3) are described on these graphs as "lines of equilibrium".

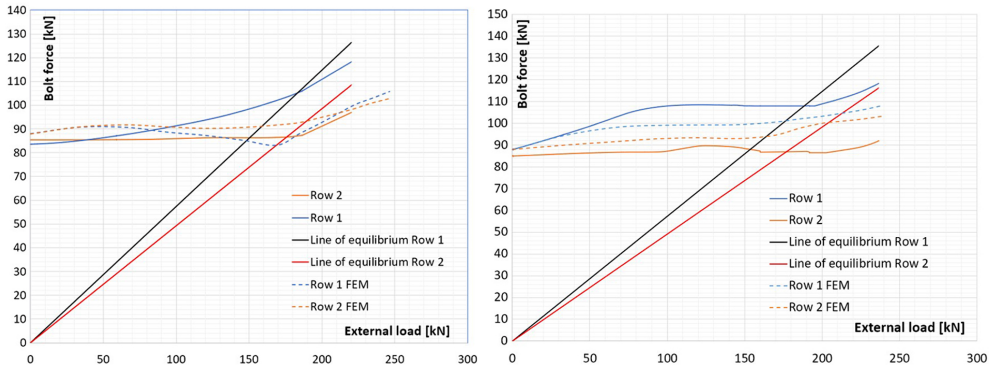


(a) (b)

Fig. 11. Bolt force vs External force diagram: a) Type A, b) Type C

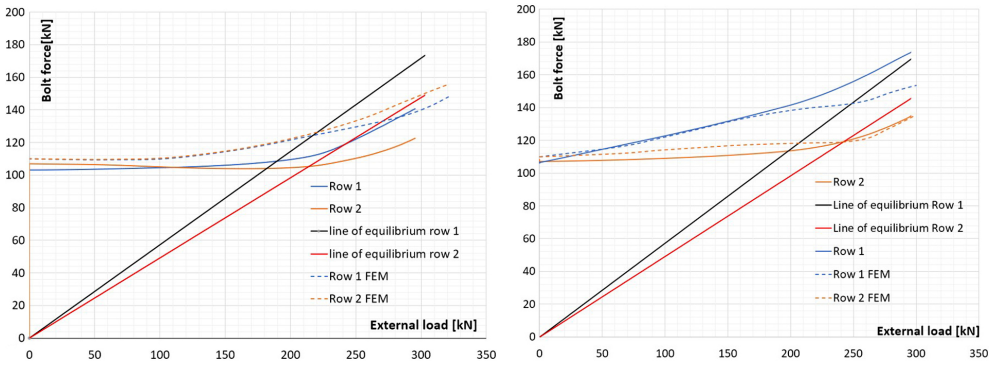


(a) (b)

Fig. 12. Bolt force vs External force diagram: a) Type B, b) Type D

After overloading the specimen with an external load of $1.55N_{0.1}$, the load was removed and the change in bolt forces was recorded. This is presented in Table 3. This is an important indicator of safety for joints prone to fatigue failure. If prestress is lost due to bolt yielding, the force amplitude in the upcoming cycles will increase, and so does risk of fatigue failure.

Table 3. Prestress load decrease upon unloading

| | **Type A** | | | **Type B** | | | **Type C** | | | **Type D** | | |
|---|---|---|---|---|---|---|---|---|---|---|---|---|
| | $F_0$ [kN] | $F_{final}$ [kN] | % | $F_0$ [kN] | $F_{final}$ [kN] | % | $F_0$ [kN] | $F_{final}$ [kN] | % | $F_0$ [kN] | $F_{final}$ [kN] | % |
| Row 1 | 85.3 | 52.6 | **–38.3** | 104.5 | 77.1 | **–26.2** | 87.9 | 44.8 | **–49.1** | 106.0 | 86.3 | **–18.6** |
| Row 2 | 83.5 | 73.7 | **–11.7** | 107.0 | 91.3 | **–14.7** | 85.1 | 47.6 | **–37.1** | 107.8 | 102.7 | **–4.7** |

Where: $F_0$ – bolt prestress force, $F_{final}$ – bolt force after unloading when $N = 0$.

In Table 4, bolt forces from FEM and from the experiment at the theoretical point of separation are presented. It should be noted, that at this point there should be little to no increase in the bolt forces (up to 20% as described in Section 1).

Table 4. Bolt force increment at the theoretical point of separation

| | **Type A** | | | **Type B** | | | **Type C** | | | **Type D** | | |
|---|---|---|---|---|---|---|---|---|---|---|---|---|
| | **$N_{0.1}$= 153 kN** | | | **$N_{0.1}$= 192 kN** | | | **$N_{0.1}$= 153 kN** | | | **$N_{0.1}$= 192 kN** | | |
| | $F_0$ [kN] | $\Delta F_0$ [kN] | % | $F_0$ [kN] | $\Delta F_0$ [kN] | % | $F_0$ [kN] | $\Delta F_0$ [kN] | % | $F_0$ [kN] | $\Delta F_0$ [kN] | % |
| Row 1 | 85.3 | TEST 98.9 | **+15.9** | 104.5 | TEST 108.7 | **+4.1** | 87.9 | TEST 108.0 | **+22.9** | 106.0 | TEST 140.1 | **+32.1** |
| | | FEM 84.0 | **–1.5** | | FEM 120.4 | **+15.2** | | FEM 99.5 | **+13.2** | | FEM 137.2 | **+29.4** |

*Continued on next page*

Table 4 – *Continued from previous page*

| | **Type A** | | | **Type B** | | | **Type C** | | | **Type D** | | |
|---|---|---|---|---|---|---|---|---|---|---|---|---|
| | $N_{0.1}$= 153 kN | | | $N_{0.1}$= 192 kN | | | $N_{0.1}$= 153 kN | | | $N_{0.1}$= 192 kN | | |
| | $F_0$ [kN] | $\Delta F_0$ [kN] | % | $F_0$ [kN] | $\Delta F_0$ [kN] | % | $F_0$ [kN] | $\Delta F_0$ [kN] | % | $F_0$ [kN] | $\Delta F_0$ [kN] | % |
| | $N_{0.2}$ = 178 kN | | | $N_{0.2}$ = 223 kN | | | $N_{0.2}$ = 178 kN | | | $N_{0.2}$ = 223 kN | | |
| Row 2 | 88.6 | TEST 86.2 | **–2.7** | 107.0 | TEST 106.2 | **–0.7** | 85.1 | TEST 81.7 | **–4.0** | 107.8 | TEST 116.3 | **+7.9** |
| | | FEM 92.2 | **+4.1** | | FEM 127.0 | **+18.6** | | FEM 96.1 | **+12.9** | | FEM 118.6 | **+10.0** |

Where: $N_{0.1}$ – theoretical load at which separation should occur for bolt row 1, $N_{0.2}$ – theoretical load at which separation should occur for bolt row 2.

# 6. Conclusions

From the results obtained from the study, the following conclusions can be formulated:

- Types A and C with fully threaded 8.8 grade bolts experienced greater losses in preload upon unloading (max. 49%), in comparison to 10.9 grade bolts (max. 26%). This can be seen in Tab. 3.
- Joint with a spacer plate (types C and D) experienced larger increases in force at the theoretical point of separation. The average force increment with a spacer plate was equal to 14.5%, while without a spacer plate, that value was equal to 4%. This can be due to the unfavourable stiffness ratio between the bolt, column flange in bending, and end plate in bending with spacer plate under compression (Eq. (1.4)). Improving spacer plate stiffness, by increasing its size, and enhancing its flatness, while reducing end plate thickness could solve this issue.
- The average difference in bolt forces at the point of separation between FEM and test results was equal to 9.7%, with 17.8% at the largest. These differences can be attributed to errors in measurements, as well as to computer modelling and input data. Plate out-of-flatness could be the reason, as perfectly flat surfaces were modelled in ANSYS.
- Finite Element Analysis also shows, that even with a very thick end plate, there is some prying action due to plate bending.
- Bolts in the second row experienced almost no increment in force before the theoretical point of separation was reached. Beyond this point, an increase was observed. It can be said that the second-row bolts responded in delay in comparison with bolts in the first row.
- 10.9-grade bolts for prestress performed better than grade 8.8 bolts not dedicated for prestress. The application of the latter requires further research.
- A spacer plate eliminates the prying effect, however, to eliminate force increments, a combination of a stiffer spacer plate with a thinner extended end plate could be used. This is where further research will be directed.

The conducted study also had some limitations. The use of two force sensors allowed to monitor only two bolts at a time. Due to many factors influencing the structural response, this did not allow to fully observe the behaviour of the connection. These factors include: plate

contact surface, plate imperfections due to welding, slightly different yield stress for individual bolts, bolt misalignment in the holes, friction, and bolt cross-talk, to mention a few. More force sensors would be required for future research. Also, the sensors' height was significant in comparison to the clamp length. Therefore, fitting in the sensors forced the use of bolts longer than in a real joint, which reduced the stiffness of the bolts. This is worth noting, as the force increment is dependent on the stiffness ratio of the joint's components. It should be underlined, that results and conclusions apply only to the scope of this research work.

## Acknowledgements

This paper was co-financed under the research grant of the Warsaw University of Technology supporting the scientific activity in the discipline of Civil Engineering, Geodesy and Transport.

## References

[1] P. Kawecki, J. Łaguna, and A. Kozłowski, "Analysis of the moment resistance of I-beam end plate connection with multiple bolt rows", *Journal of Civil Engineering, Environment and Architecture*, vol. 21, no. 2, pp. 117–136, 2013, doi: 10.7862/rb.2013.21 (in Polish).

[2] K. Ostrowski, J. Łaguna, and A. Kozłowski, "Weryfikacja efektu dźwigni w rozciąganym połączeniu doczołowym sprężonym śrubami", *Budownictwo i Architektura*, vol. 12, no. 2, pp. 251–258, 2013.

[3] EN 1993-1-8:2005 Eurocode 3: Design of steel structures – Part 1–8: Design of joints. CEN, 2005.

[4] W. Kawecki, P. Kawecki, A. Klimek, and J. Łaguna, "Uproszczona procedura projektowania sztywnych doczołowych połączeń sprężanych na podstawie PN-EN 1993-1-8", *Inżynieria i Budownictwo*, vol. 65, no. 7, pp. 393–398, 2009.

[5] A. Biegus, *Połączenia śrubowe*. Warszawa-Wrocław: Wydawnictwo Naukowe PWN, 1997.

[6] PN-90/B-03200 Konstrukcje Stalowe, Obliczenia statyczne i projektowanie. PKN, 1990.

[7] G.L. Kulak, J.W. Fisher, and J.H.A. Struik, *Guide to Design Criteria for Bolted and Riveted Joints*, 2nd ed. Chicago: American Institute of Steel Construction, 2001.

[8] J. Bródka, A. Kozłowski, I. Ligocki, J. Łaguna, and L. Ślęczka, *Projektowanie i obliczanie połączeń i węzłów konstrukcji stalowych*, vol. 1. Rzeszów: Polskie Wydawnictwo Techniczne, 2013.

[9] C.G. Salmon and J.E. Johnson, *Steel Structures, Design and Behavior*, 2nd ed. New York: Harper and Row, 1980.

[10] R.S. Nair, P.C. Birkemoe, and W.H. Munse, "High Strength Bolts Subjected to Tension and Prying", *Journal of the Structural Division*, ASCE, vol. 100, no. 2, pp. 351–372, 1974.

[11] G. Owens and B.D. Cheal, *Structural Steelwork Connections.* London: Butterworths, 1989.

[12] R.G. Budynas and J.K. Nisbett, *Shigley's Mechanical Engineering Design*. New York: McGraw-Hill Education, 2020.

[13] EN 10025-2:2019 Hot rolled products of structural steels – technical delivery conditions for non-alloy structural steels. CEN, 2019.

[14] ISO 4017:2022 Fasteners – Hexagon head screws – Product grades A and B. ISO, 2022.

[15] ISO 4032:2023 Hexagon regular nuts (style 1) – Product grades A and B. ISO, 2023.

[16] EN 14399-4:2006 High-strength structural bolting assemblies for preloading – Part 4: System HV – Hexagon bolt and nut assemblies. CEN, 2006.

[17] "KMRplus Force Washer", HBK. [Online]. Available: https://www.hbm.com/en/8261/kmrplus-force-washer/?product_type_no=KMRplus%20Strain%20Gauge-Based%20Force%20Washer.

[18] ISO 898-1:2013 Mechanical properties of fasteners made of carbon steel and alloy steel Part 1: Bolts, screws and studs with specified property classes – Coarse thread and fine pitch thread. ISO, 2013.

[19] X. Yun and L. Gardner, "Stress-strain curves for hot-rolled steels", *Journal of Constructional Steel Research*, vol. 133, pp. 36–46, 2017, doi: 10.1016/j.jcsr.2017.01.024.

## Badania doświadczalne połączenia z blachą czołową i sprężonymi śrubami

**Słowa kluczowe:** śruba, sprężenie, MES, ANSYS Workbench, przekładka dystansowa, efekt dźwigni

### Streszczenie:

Ta praca przedstawia wyniki badań doświadczalnym zginanego połączenia z blachą czołową i sprężonymi śrubami. Zmierzono i porównano przyrosty sił w śrubach pod obciążeniem, dla dwóch rozwiązań mających na celu im zapobiegać. Pierwsze z nich zakłada grubą blachę czołową, celem zmniejszenia efektu dźwigni, a drugie wprowadza do połączenia przekładkę dystansową, aby całkowicie wyeliminować ten efekt całkowicie. Ograniczenie przyrostów sił w śrubach jest kluczowe w projektowaniu połączeń pracujących pod obciążeniem cyklicznym, które są narażone na zniszczenie zmęczeniowe. Przebadano cztery typy połączeń, gdzie dwa z nich posiadały przekładkę dystansową między blachą czołową a pasem słupa. Użyto śrub M16 klasy 8.8 i 10.9. Belkę wykonano z profilu IPE 400, a słup z profilu HEB 220 – oba ze stali gatunku S355-J2. Przebadano możliwość użycia śrub nie przeznaczonych do sprężania. Przeprowadzono analizę MES w programie ANSYS Workbench. Wyniki podsumowano poddano dyskusji.

Received: 2024-12-31, Revised: 2025-04-15